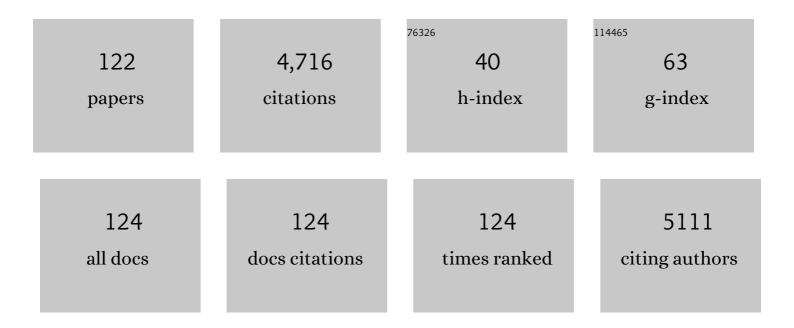
List of Publications by Year in descending order

Source: https://exaly.com/author-pdf/6789620/publications.pdf Version: 2024-02-01



#	Article	IF	CITATIONS
1	Tailoring the metal-perovskite interface for promotional steering of the catalytic NO reduction by CO in the presence of H2O on Pd-lanthanum iron manganite composites. Applied Catalysis B: Environmental, 2022, 307, 121160.	20.2	11
2	Dry Reforming of Methane on NiCu and NiPd Model Systems: Optimization of Carbon Chemistry. Catalysts, 2022, 12, 311.	3.5	11
3	The state of zinc in methanol synthesis over a Zn/ZnO/Cu(211) model catalyst. Science, 2022, 376, 603-608.	12.6	65
4	Who Does the Job? How Copper Can Replace Noble Metals in Sustainable Catalysis by the Formation of Copper–Mixed Oxide Interfaces. ACS Catalysis, 2022, 12, 7696-7708.	11.2	7
5	Steering the Methane Dry Reforming Reactivity of Ni/La ₂ O ₃ Catalysts by Controlled In Situ Decomposition of Doped La ₂ NiO ₄ Precursor Structures. ACS Catalysis, 2021, 11, 43-59.	11.2	38
6	The sol–gel autocombustion as a route towards highly CO ₂ -selective, active and long-term stable Cu/ZrO ₂ methanol steam reforming catalysts. Materials Chemistry Frontiers, 2021, 5, 5093-5105.	5.9	12
7	Mechanistic in situ insights into the formation, structural and catalytic aspects of the La2NiO4 intermediate phase in the dry reforming of methane over Ni-based perovskite catalysts. Applied Catalysis A: General, 2021, 612, 117984.	4.3	16
8	Operando Fourier-transform infrared–mass spectrometry reactor cell setup for heterogeneous catalysis with glovebox transfer process to surface-chemical characterization. Review of Scientific Instruments, 2021, 92, 024105.	1.3	8
9	Steering the methanol steam reforming performance of Cu/ZrO2 catalysts by modification of the Cu-ZrO2 interface dimensions resulting from Cu loading variation. Applied Catalysis A: General, 2021, 623, 118279.	4.3	13
10	In Situ-Determined Catalytically Active State of LaNiO ₃ in Methane Dry Reforming. ACS Catalysis, 2020, 10, 1102-1112.	11.2	55
11	Carbide-Modified Pd on ZrO2 as Active Phase for CO2-Reforming of Methane—A Model Phase Boundary Approach. Catalysts, 2020, 10, 1000.	3.5	14
12	Mechanistic insights into the catalytic methanol steam reforming performance of Cu/ZrO2 catalysts by in situ and operando studies. Journal of Catalysis, 2020, 391, 497-512.	6.2	41
13	Increasing Complexity Approach to the Fundamental Surface and Interface Chemistry on SOFC Anode Materials. Accounts of Chemical Research, 2020, 53, 1811-1821.	15.6	2
14	Spectro-electrochemical setup for in situ and operando mechanistic studies on metal oxide electrode surfaces. Review of Scientific Instruments, 2020, 91, 084104.	1.3	3
15	Treading in the Limited Stability Regime of Lanthanum Strontium Ferrite — Reduction, Phase Change and Exsolution. ECS Transactions, 2019, 91, 1771-1781.	0.5	4
16	Promotion of La(Cu0.7Mn0.3)0.98M0.02O3â~ʾδ (M = Pd, Pt, Ru and Rh) perovskite catalysts by noble metals for the reduction of NO by CO. Journal of Catalysis, 2019, 379, 18-32.	6.2	32
17	Crystallographic and electronic evolution of lanthanum strontium ferrite (La _{0.6} Sr _{0.4} FeO _{3â^îr}) thin film and bulk model systems during iron exsolution. Physical Chemistry Chemical Physics, 2019, 21, 3781-3794.	2.8	18
18	On the structural stability of crystalline ceria phases in undoped and acceptor-doped ceria materials under <i>in situ</i> reduction conditions. CrystEngComm, 2019, 21, 145-154.	2.6	32

#	Article	IF	CITATIONS
19	Reactive metal-support interaction in the Cu-In ₂ O ₃ system: intermetallic compound formation and its consequences for CO ₂ -selective methanol steam reforming. Science and Technology of Advanced Materials, 2019, 20, 356-366.	6.1	26
20	CO ₂ Reduction by Hydrogen Preâ€Reduced Acceptorâ€Doped Ceria. ChemPhysChem, 2019, 20, 1706-1718.	2.1	7
21	An ultra-flexible modular high vacuum setup for thin film deposition. Review of Scientific Instruments, 2019, 90, 023902.	1.3	5
22	Structural and kinetic aspects of CO oxidation on ZnOx-modified Cu surfaces. Applied Catalysis A: General, 2019, 572, 151-157.	4.3	16
23	Substoichiometric zirconia thin films prepared by reactive sputtering of metallic zirconium using a direct current ion beam source. Surface Science, 2019, 680, 52-60.	1.9	6
24	Role of Precursor Carbides for Graphene Growth on Ni(111). Scientific Reports, 2018, 8, 2662.	3.3	13
25	Structural investigations of La _{0.6} Sr _{0.4} FeO _{3â^î^} under reducing conditions: kinetic and thermodynamic limitations for phase transformations and iron exsolution phenomena. RSC Advances, 2018, 8, 3120-3131.	3.6	37
26	CO ₂ Reduction on the Preâ€reduced Mixed Ionic–Electronic Conducting Perovskites La _{0.6} Sr _{â€0.4} FeO _{3â€Î′} and SrTi _{0.7} Fe _{0.3} O _{3â€Î′} . ChemPhysChem, 2018, 19, 93-107.	2.1	8
27	The Chemical Evolution of the La0.6Sr0.4CoO3â^δSurface Under SOFC Operating Conditions and Its Implications for Electrochemical Oxygen Exchange Activity. Topics in Catalysis, 2018, 61, 2129-2141.	2.8	65
28	Zirconiumâ€assistierte Aktivierung von Palladium zur Steigerung der Produktion von Synthesegas in der Trockenreformierung von Methan. Angewandte Chemie, 2018, 130, 14823-14828.	2.0	3
29	Zirconiumâ€Assisted Activation of Palladium To Boost Syngas Production by Methane Dry Reforming. Angewandte Chemie - International Edition, 2018, 57, 14613-14618.	13.8	44
30	Water adsorption at zirconia: from the ZrO ₂ (111)/Pt ₃ Zr(0001) model system to powder samples. Journal of Materials Chemistry A, 2018, 6, 17587-17601.	10.3	24
31	Impregnated and Co-precipitated Pd–Ga2O3, Pd–In2O3 and Pd–Ga2O3–In2O3 Catalysts: Influence of th Microstructure on the CO2 Selectivity in Methanol Steam Reforming. Catalysis Letters, 2018, 148, 3062-3071.	e 2.6	21
32	Complex oxide thin films: Pyrochlore, defect fluorite and perovskite model systems for structural, spectroscopic and catalytic studies. Applied Surface Science, 2018, 452, 190-200.	6.1	12
33	H2 reduction of Gd- and Sm-doped ceria compared to pure CeO2 at high temperatures: effect on structure, oxygen nonstoichiometry, hydrogen solubility and hydroxyl chemistry. Physical Chemistry Chemical Physics, 2018, 20, 22099-22113.	2.8	12
34	Surface composition changes of CuNi-ZrO2 during methane decomposition: An operando NAP-XPS and density functional study. Catalysis Today, 2017, 283, 134-143.	4.4	48
35	Surface chemistry of pure tetragonal ZrO ₂ and gas-phase dependence of the tetragonal-to-monoclinic ZrO ₂ transformation. Dalton Transactions, 2017, 46, 4554-4570.	3.3	31
36	Surface Chemistry of Perovskite-Type Electrodes During High Temperature CO ₂ Electrolysis Investigated by <i>Operando</i> Photoelectron Spectroscopy. ACS Applied Materials & Interfaces, 2017, 9, 35847-35860.	8.0	107

#	Article	IF	CITATIONS
37	Structural and Catalytic Properties of Ag- and Co ₃ O ₄ -Impregnated Strontium Titanium Ferrite SrTi _{0.7} Fe _{0.3} O _{3â~Î} in Methanol Steam Reforming. Industrial & Engineering Chemistry Research, 2017, 56, 13654-13662.	3.7	6
38	A Comparative Discussion of the Catalytic Activity and CO2-Selectivity of Cu-Zr and Pd-Zr (Intermetallic) Compounds in Methanol Steam Reforming. Catalysts, 2017, 7, 53.	3.5	24
39	Rhodium atalyzed Methanation and Methane Steam Reforming Reactions on Rhodium–Perovskite Systems: Metal–Support Interaction. ChemCatChem, 2016, 8, 2057-2067.	3.7	25
40	From zirconia to yttria: Sampling the YSZ phase diagram using sputter-deposited thin films. AIP Advances, 2016, 6, .	1.3	49
41	Microstructural and Chemical Evolution and Analysis of a Self-Activating CO ₂ -Selective Cu–Zr Bimetallic Methanol Steam Reforming Catalyst. Journal of Physical Chemistry C, 2016, 120, 25395-25404.	3.1	19
42	Structural and chemical degradation mechanisms of pure YSZ and its components ZrO2 and Y2O3 in carbon-rich fuel gases. Physical Chemistry Chemical Physics, 2016, 18, 14333-14349.	2.8	11
43	High-Temperature Carbon Deposition on Oxide Surfaces by CO Disproportionation. Journal of Physical Chemistry C, 2016, 120, 1795-1807.	3.1	32
44	Tuning of the copper–zirconia phase boundary for selectivity control of methanol conversion. Journal of Catalysis, 2016, 339, 111-122.	6.2	20
45	Structure–Property Relationships in the Y2O3–ZrO2 Phase Diagram: Influence of the Y-Content on Reactivity in C1 Gases, Surface Conduction, and Surface Chemistry. Journal of Physical Chemistry C, 2016, 120, 22443-22454.	3.1	4
46	Evidence for dissolved hydrogen in the mixed ionic–electronic conducting perovskites La _{0.6} Sr _{0.4} FeO _{3â~îî} and SrTi _{0.7} Fe _{0.3} O _{3â~îî} . Physical Chemistry Chemical Physics, 2016, 18, 26873-26884.	2.8	4
47	Chemical vapor deposition-prepared sub-nanometer Zr clusters on Pd surfaces: promotion of methane dry reforming. Physical Chemistry Chemical Physics, 2016, 18, 31586-31599.	2.8	15
48	Structural and Electrochemical Properties of Physisorbed and Chemisorbed Water Layers on the Ceramic Oxides Y2O3, YSZ, and ZrO2. ACS Applied Materials & Interfaces, 2016, 8, 16428-16443.	8.0	41
49	Boosting Hydrogen Production from Methanol and Water by in situ Activation of Bimetallic Cuâ^'Zr Species. ChemCatChem, 2016, 8, 1778-1781.	3.7	16
50	Surface Reactivity of YSZ, Y ₂ O ₃ , and ZrO ₂ toward CO, CO ₂ , and CH ₄ : A Comparative Discussion. Journal of Physical Chemistry C, 2016, 120, 3882-3898.	3.1	23
51	Ambient Pressure XPS Study of Mixed Conducting Perovskite-Type SOFC Cathode and Anode Materials under Well-Defined Electrochemical Polarization. Journal of Physical Chemistry C, 2016, 120, 1461-1471.	3.1	132
52	Ni–perovskite interaction and its structural and catalytic consequences in methane steam reforming and methanation reactions. Journal of Catalysis, 2016, 337, 26-35.	6.2	56
53	Distinct carbon growth mechanisms on the components of Ni/YSZ materials. Materials Chemistry and Physics, 2016, 173, 508-515.	4.0	10
54	Enhancing Electrochemical Waterâ€Splitting Kinetics by Polarizationâ€Driven Formation of Nearâ€Surface Iron(0): An Inâ€Situ XPS Study on Perovskiteâ€Type Electrodes. Angewandte Chemie, 2015, 127, 2666-2670.	2.0	12

#	Article	IF	CITATIONS
55	Frontispiz: Enhancing Electrochemical Water-Splitting Kinetics by Polarization-Driven Formation of Near-Surface Iron(0): An Inâ€Situ XPS Study on Perovskite-Type Electrodes. Angewandte Chemie, 2015, 127, n/a-n/a.	2.0	0
56	Near-Ambient-Pressure X-ray Photoelectron Spectroscopy Study of Methane-Induced Carbon Deposition on Clean and Copper-Modified Polycrystalline Nickel Materials. Journal of Physical Chemistry C, 2015, 119, 26948-26958.	3.1	10
57	Preparation and characterization of epitaxially grown unsupported yttria-stabilized zirconia (YSZ) thin films. Applied Surface Science, 2015, 331, 427-436.	6.1	15
58	Frontispiece: Enhancing Electrochemical Water-Splitting Kinetics by Polarization-Driven Formation of Near-Surface Iron(0): An Inâ€Situ XPS Study on Perovskite-Type Electrodes. Angewandte Chemie - International Edition, 2015, 54, n/a-n/a.	13.8	0
59	Steering of methanol reforming selectivity by zirconia–copper interaction. Journal of Catalysis, 2015, 321, 123-132.	6.2	26
60	Enhancing Electrochemical Waterâ€Splitting Kinetics by Polarizationâ€Driven Formation of Nearâ€Surface Iron(0): An Inâ€Situ XPS Study on Perovskiteâ€Type Electrodes. Angewandte Chemie - International Edition, 2015, 54, 2628-2632.	13.8	110
61	Water-Gas Shift and Methane Reactivity on Reducible Perovskite-Type Oxides. Journal of Physical Chemistry C, 2015, 119, 11739-11753.	3.1	19
62	Trimethylaluminum and Oxygen Atomic Layer Deposition on Hydroxyl-Free Cu(111). ACS Applied Materials & Interfaces, 2015, 7, 16428-16439.	8.0	39
63	Exsolution of Fe and SrO Nanorods and Nanoparticles from Lanthanum Strontium Ferrite La _{0.6} Sr _{0.4} FeO _{3â~Î<} Materials by Hydrogen Reduction. Journal of Physical Chemistry C, 2015, 119, 22050-22056.	3.1	52
64	Surface modification processes during methane decomposition on Cu-promoted Ni–ZrO ₂ catalysts. Catalysis Science and Technology, 2015, 5, 967-978.	4.1	48
65	Enhanced Kinetic Stability of Pure and Y-Doped Tetragonal ZrO ₂ . Inorganic Chemistry, 2014, 53, 13247-13257.	4.0	34
66	A high-temperature, ambient-pressure ultra-dry operando reactor cell for Fourier-transform infrared spectroscopy. Review of Scientific Instruments, 2014, 85, 084102.	1.3	24
67	The catalytic properties of thin film Pd-rich GaPd2 in methanol steam reforming. Journal of Catalysis, 2014, 309, 231-240.	6.2	29
68	Combined UHV/high-pressure catalysis setup for depth-resolved near-surface spectroscopic characterization and catalytic testing of model catalysts. Review of Scientific Instruments, 2014, 85, 055104.	1.3	15
69	Hydrogen Surface Reactions and Adsorption Studied on Y ₂ O ₃ , YSZ, and ZrO ₂ . Journal of Physical Chemistry C, 2014, 118, 8435-8444.	3.1	50
70	Methane Decomposition and Carbon Growth on Y ₂ O ₃ , Yttria-Stabilized Zirconia, and ZrO ₂ . Chemistry of Materials, 2014, 26, 1690-1701.	6.7	44
71	In Situ FT-IR Spectroscopic Study of CO ₂ and CO Adsorption on Y ₂ O ₃ , ZrO ₂ , and Yttria-Stabilized ZrO ₂ . Journal of Physical Chemistry C, 2013, 117, 17666-17673.	3.1	268
72	Kinetics of Palladium Oxidation in the mbar Pressure Range: Ambient Pressure XPS Study. Topics in Catalysis, 2013, 56, 885-895.	2.8	35

#	Article	IF	CITATIONS
73	Electron microscopy investigations of metal-support interaction effects in M/Y2O3 and M/ZrO2 thin films (M=Cu, Ni). Materials Chemistry and Physics, 2013, 143, 167-177.	4.0	2
74	An (ultra) high-vacuum compatible sputter source for oxide thin film growth. Review of Scientific Instruments, 2013, 84, 094103.	1.3	14
75	ZnO is a CO 2 -selective steam reforming catalyst. Journal of Catalysis, 2013, 297, 151-154.	6.2	59
76	Formation and stability of small well-defined Cu- and Ni oxide particles. Materials Chemistry and Physics, 2013, 143, 184-194.	4.0	3
77	Thin film model systems of ZrO2 and Y2O3 as templates for potential industrial applications investigated by means of electron microscopy. Materials Chemistry and Physics, 2013, 138, 384-391.	4.0	5
78	Methanol steam reforming: CO2-selective Pd2Ga phases supported on α- and γ-Ga2O3. Applied Catalysis A: General, 2013, 453, 34-44.	4.3	24
79	From Oxideâ€5upported Palladium to Intermetallic Palladium Phases: Consequences for Methanol Steam Reforming. ChemCatChem, 2013, 5, 1273-1285.	3.7	41
80	Alloying and Structure of Ultrathin Gallium Films on the (111) and (110) Surfaces of Palladium. Journal of Physical Chemistry C, 2013, 117, 19558-19567.	3.1	3
81	CO2-selective methanol steam reforming on In-doped Pd studied by in situ X-ray photoelectron spectroscopy. Journal of Catalysis, 2012, 295, 186-194.	6.2	53
82	Growth and Alloying of Ultra-Thin Zn Layers on Pd(110). Journal of Physical Chemistry C, 2012, 116, 3635-3644.	3.1	10
83	Reduction of Different GeO ₂ Polymorphs. Journal of Physical Chemistry C, 2012, 116, 9961-9968.	3.1	16
84	Hydrogen Production by Methanol Steam Reforming on Copper Boosted by Zincâ€Assisted Water Activation. Angewandte Chemie - International Edition, 2012, 51, 3002-3006.	13.8	79
85	How to Control the Selectivity of Palladiumâ€based Catalysts in Hydrogenation Reactions: The Role of Subsurface Chemistry. ChemCatChem, 2012, 4, 1048-1063.	3.7	223
86	In situ XPS study of methanol reforming on PdGa near-surface intermetallic phases. Journal of Catalysis, 2012, 290, 126-137.	6.2	48
87	Quantum mechanical calculations of the vibrational spectra of quartz- and rutile-type GeO2. Physics and Chemistry of Minerals, 2012, 39, 47-55.	0.8	32
88	A High-Resolution Diffraction and Spectroscopic Study of the Low-Temperature Phase Transformation of Hexagonal to Tetragonal GeO2 with and without Alkali Hydroxide Promotion. Journal of Physical Chemistry C, 2011, 115, 9706-9712.	3.1	20
89	Preparation and structural characterization of SnO2 and GeO2 methanol steam reforming thin film model catalysts by (HR)TEM. Materials Chemistry and Physics, 2010, 122, 623-629.	4.0	25
90	Steam reforming of methanol on PdZn near-surface alloys on Pd(1 1 1) and Pd foil studied by in-situ XPS, LEIS and PM-IRAS. Journal of Catalysis, 2010, 276, 101-113.	6.2	68

#	Article	IF	CITATIONS
91	Subsurfaceâ€Controlled CO ₂ Selectivity of PdZn Nearâ€Surface Alloys in H ₂ Generation by Methanol Steam Reforming. Angewandte Chemie - International Edition, 2010, 49, 3224-3227.	13.8	144
92	Pd–In2O3 interaction due to reduction in hydrogen: Consequences for methanol steam reforming. Applied Catalysis A: General, 2010, 374, 180-188.	4.3	82
93	Origin of different deactivation of Pd/SnO2 and Pd/GeO2 catalysts in methanol dehydrogenation and reforming: A comparative study. Applied Catalysis A: General, 2010, 381, 242-252.	4.3	24
94	Catalytic characterization of pure SnO2 and GeO2 in methanol steam reforming. Applied Catalysis A: General, 2010, 375, 188-195.	4.3	23
95	Hydrogen on In ₂ O ₃ : Reducibility, Bonding, Defect Formation, and Reactivity. Journal of Physical Chemistry C, 2010, 114, 9022-9029.	3.1	106
96	Dendritic growth of amorphous gallium oxide in mixed GaOx/WOx thin films. Materials Chemistry and Physics, 2009, 116, 175-182.	4.0	6
97	Growth, thermal stability and structure of ultrathin Zn-layers on Pd(111). Surface Science, 2009, 603, 251-255.	1.9	36
98	Pd/Ga2O3 methanol steam reforming catalysts: Part I. Morphology, composition and structural aspects. Applied Catalysis A: General, 2009, 358, 193-202.	4.3	71
99	Pd/Ga2O3 methanol steam reforming catalysts: Part II. Catalytic selectivity. Applied Catalysis A: General, 2009, 358, 203-210.	4.3	51
100	The structure and composition of oxidized and reduced tungsten oxide thin films. Thin Solid Films, 2008, 516, 2829-2836.	1.8	42
101	Growth and stability of Ga2O3 nanospheres. Thin Solid Films, 2008, 516, 4742-4749.	1.8	26
102	Novel methanol steam reforming activity and selectivity of pure In2O3. Applied Catalysis A: General, 2008, 347, 34-42.	4.3	81
103	Defect formation and the water–gas shift reaction on β-Ga2O3. Journal of Catalysis, 2008, 256, 278-286.	6.2	37
104	Hydrogen on polycrystalline β-Ga2O3: Surface chemisorption, defect formation, and reactivity. Journal of Catalysis, 2008, 256, 268-277.	6.2	62
105	A New Preparation Pathway to Well-Defined In2O3Nanoparticles at Low Substrate Temperatures. Journal of Physical Chemistry C, 2008, 112, 918-925.	3.1	23
106	Methane Oxidation on Pd(111):  In Situ XPS Identification of Active Phase. Journal of Physical Chemistry C, 2007, 111, 7957-7962.	3.1	81
107	Structural and redox properties of VOxand Pd/VOxthin film model catalysts studied by TEM and SAED. Physical Chemistry Chemical Physics, 2007, 9, 2428-2433.	2.8	8
108	Comparison of the reactivity of different Pd–O species in CO oxidation. Physical Chemistry Chemical Physics, 2007, 9, 533-540.	2.8	92

#	Article	IF	CITATIONS
109	Ethene Oxidation on Pd(111): Kinetic Hysteresis Induced by Carbon Dissolution. Catalysis Letters, 2007, 119, 191-198.	2.6	6
110	Carbon Incorporation in Pd(111) by Adsorption and Dehydrogenation of Ethene. Journal of Physical Chemistry B, 2006, 110, 4947-4952.	2.6	60
111	Zn Adsorption on Pd(111):Â ZnO and PdZn Alloy Formation. Journal of Physical Chemistry B, 2006, 110, 11391-11398.	2.6	48
112	Growth and decay of the Pd(111)–Pd5O4 surface oxide: Pressure-dependent kinetics and structural aspects. Surface Science, 2006, 600, 205-218.	1.9	57
113	In situ XPS study of Pd(111) oxidation. Part 1: 2D oxide formation in 10â^'3mbar O2. Surface Science, 2006, 600, 983-994.	1.9	142
114	In situ XPS study of Pd(111) oxidation at elevated pressure, Part 2: Palladium oxidation in the 10â^'1mbar range. Surface Science, 2006, 600, 2980-2989.	1.9	146
115	Hydrogen-induced metal-oxide interaction studied on noble metal model catalysts. Reaction Kinetics and Catalysis Letters, 2006, 87, 215-234.	0.6	9
116	Growth and structural stability of well-ordered PdZn alloy nanoparticles. Journal of Catalysis, 2006, 241, 14-19.	6.2	78
117	Carbon incorporation during ethene oxidation on Pd(111) studied by in situ X-ray photoelectron spectroscopy at 2×10â^'3Âmbar2×10â^'3Âmbar. Journal of Catalysis, 2006, 242, 340-348.	6.2	41
118	Growth and decomposition of aligned and ordered PdO nanoparticles. Journal of Chemical Physics, 2006, 125, 094703.	3.0	58
119	Catalytic Oxidation of Ethene on Polycrystalline Palladium: Influence of the Oxidation State of the Surface. Catalysis Letters, 2005, 104, 1-8.	2.6	15
120	Adsorption and hydrogenation of CO on Pd() and Rh() modified by subsurface vanadium. Surface Science, 2003, 532-535, 142-147.	1.9	31
121	Oxygen-induced surface phase transformation of Pd(1 1 1): sticking, adsorption and desorption kinetics. Surface Science, 2001, 482-485, 237-242.	1.9	60
122	Title is missing!. Topics in Catalysis, 2000, 14, 25-33.	2.8	28